Hydrol. Earth Syst. Sci. Discuss., 8, 7293–7317, 2011
www.hydrol-earth-syst-sci-discuss.net/8/7293/2011/
doi:10.5194/hessd-8-7293-2011

Hydrology and Earth System Sciences Discussions

Assessing water resources in China using PRECIS projections and VIC model

G. Q. Wang[1,2], J. Y. Zhang[1,2], J. L. Jin[1,2], T. C. Pagano[3], R. Calow[4], Z. X. Bao[1,2], C. S Liu[1,2], Y. L. Liu[1,2], and X. L. Yan[1,2]

[1]Nanjing Hydraulic Research Institute, Nanjing 210029, China
[2]Research Center for Climate Change, Ministry of Water Resources, Nanjing 210029, China
[3]CSIRO Land and Water, Melbourne, Victoria, Australia
[4]Overseas Development Institute, London SE1 7JD, UK

Received: 17 June 2011 – Accepted: 12 July 2011 – Published: 25 July 2011

Correspondence to: G. Q. Wang (gqwang@nhri.cn)

Published by Copernicus Publications on behalf of the European Geosciences Union.

Abstract

Climate change is now a major environmental and developmental issue, and one that will increase the challenge of sustainable water resources management. In order to assess the implications of climate change on water resources in China, a Variable Infiltration Capacity (VIC) model with a resolution of $50 \times 50\,km^2$ was calibrated using data from 125 well gauged catchments. According to similarities in climate conditions, soil texture and other variables, model parameters were transferred to other areas not covered by the calibrated catchments. Taking runoff in the period 1961 ~ 1990 as a baseline, the impact of climate change on runoff under three emissions scenarios of A2, B2 and A1B was studied. Model findings indicate that annual runoff over China as a whole will probably increase by approximately 3 ~ 10 % by 2050, but with quite uneven spatial and temporal distribution. The prevailing pattern of "north dry and south wet" in China is likely to be exacerbated under global warming.

1 Introduction

Global warming caused by increasing atmospheric concentration of carbon dioxide and other trace gases has become evident. A broad consensus has concluded that the earth surface air temperature increased by about 0.74° during the last century, with and temperature increases were greatest during the 1990s. Moreover, global temperature increases are likely to persist in the 21st century and will probably be accompanied by changes in precipitation (IPCC, 2007).

In China, changes in surface air temperature are similar to those experienced globally, with increases of about 0.5 ~ 0.8° during the last century, slightly exceeding global temperature change in this period. Over the last 50 yr, air temperature increased by 1.1°, with the warmest decade occurring in the 1990s. Northeast China, north China, and northwest China experienced significant warming in terms of annual average temperatures, with most warming occurring in winter and spring, as expected. In contrast, there has been no significant long term change in country-averaged annual

precipitation. However, an obvious drying trend in the Yellow River basin and significant wetting in the Yangtze River basin were detectable over the last 50 yr to the twentieth century (Ding, 2006). Global warming is likely to change precipitation patterns and probably raise the frequency of extreme events.

Climate change and greater climate variability is expected to alter the timing and magnitude of runoff, with significant implications for water resources, water infrastructure and water resources management. Competition for water at different scales, and between different uses and users, is increasing rapidly; floods and drought remain major economic as well as social issues; and environmental issues around water quality and quantity rank high amongst public (and political) concerns. Developing a better understanding of the impact of climate change on water systems in China is therefore a high priority.

Water resources and climate change have been widely investigated and documented throughout the world. An important way of assessing the likely impacts of climate change on water resources is to apply climate change scenarios to dive rainfall runoff models to estimate runoff and stream flow. Conceptual watershed models are often believed to be useful in assessing the impact of climate change on regional hydrology (Arnell, 1999; Zhang, et al., 2007). Gleick (1987) developed a monthly water balance model specifically for climate change impact assessment and addressed the advantage of using conceptual watershed models in practice (Gleick et al., 1987). Athanasios Loukas (1996) applied a UBC watershed model to study the effects of climate change on the hydrological regime of two climatically different British Columbia watersheds, the Upper Campbell and Illecilewaet watersheds (Athanasios et al., 1996). Huntington (2006) investigated relations between mean annual temperature, annual precipitation and evapotranspiration (ET) for 38 forested watersheds in New England, USA, and concluded climate warming could reduce runoff significantly (Huntington, 2006). Roger N. Jones estimated sensitivities of mean annual runoff in 22 Australian catchments to climate change using selected hydrological models, showing how results varied between models (Roger et al., 2005). Using ArcGIS Geostatistical Analyst et al. (2007)

developed a method to study the impacts of climate change on regional hydrological regimes in the Spokane River watershed. His study indicated that a 30 % increase in precipitation could result in a 50 % increase in stream flow; conversely, a 20 % decrease in precipitation could results in a 25∼30 % reduction in stream flow (Fu et al., 2007). Using a NAM model, Thodsen (2006) investigated the influence of climate change on river discharge in five major Danish rivers for the future period of 2071 ∼ 2100, 12 % increase in runoff is founded (Hans, 2006). In China et al. (2008) projected approximately 5 % decrease in runoff for the head region of the Yellow River with an improved XAJ model and ensemble projections of Global Climate Models (GCMs) used in IPCC AR4 (Li et al., 2008). Zhang (2009) assessed hydrological responses of the Yellow River to hypothetical climate scenarios using a snowmelt-based water balance model, demonstrating the role soil and water conservations measures could play in reducing the sensitivity of runoff to climate change (Zhang et al., 2009).

The IPCC (Intergovernmental Panel on Climate Change, IPCC) has reviewed and referenced the latest studies on climate change and water resources, ranging from local to continental scales, and representing a wide variety of physiographic conditions (IPCC, 2008). Previous studies indicate that stream flow is highly sensitive to changes in precipitation, as well as to changes in temperature. A 10 % change in precipitation, all other things being equal, can result in a 12 % ∼ 25 % change in runoff, a 2 degree rise in temperature can lead to a 5 % ∼ 12 % decrease in runoff; and runoff in semi-arid or arid areas is more sensitive to climate change than runoff in humid areas (Zhang et al., 2007, 2009; IPCC, 2008). The majority of studies have a catchment focus. National studies, including China, have been rare because of variable climate conditions, land cover, morphology and topography.

The objectives of this study are to (1) develop a national model for the purpose of climate change impact assessment in China, (2) to investigate climate change scenarios over the China, and (3) to explore the likely impact of climate change on water resources. Figure 1 shows the location of the ten major river basins in China covered by the study.

2 Data and methods

2.1 Description of VIC model

The VIC model (Variable Infiltration Capacity, VIC) is used to simulate the physical exchange processes of water and energy in the soil, vegetation and atmosphere in a surface vegetation atmospheric transfer scheme. It was developed by Liang et al. (1994) and later improved by Lohmann et al. (1998) and Liang and Xie (2001). The notable characteristics of the VIC model are that it includes: (1) both water balance and energy balance parameterization; (2) two types of runoff yielding mechanisms based on saturation and infiltration excess; (3) consideration of sub-grid scale soil heterogeneity; and (4) processes of snow accumulation and melt, as well as soil freezing and thawing.

The VIC model divides study catchments into grid cells and the soil column of each grid into three layers. The upper two layers, designed to represent the dynamic response of soil to rainfall events, were usually used as one layer. The lower soil layer is used to characterize the behavior of seasonal soil moisture. Three types of evaporation are considered: (1) evaporation from wet canopy; (2) evapotranspiration from dry canopy; and (3) evaporation from bare soil. Stoma resistance is used to reflect the effect of radiation, soil moisture, vapor pressure deficiency, air temperature and other factors when calculating transpiration from the canopy.

The total runoff estimates consist of surface flow and base flow. Surface flow, including infiltration excess flow and saturation excess flow, is generated in the two top layers only. In order to consider the heterogeneity of soil properties, soil storage capacity distribution curve and infiltration capacity curve were employed. The double curves are individually described as power functions with a parameter B as exponent. Base flow occurs in the lowest layer only and is described using the ARNO method (Habets, 1999). A one dimensional Richards equation is used to describe the vertical soil moisture movement.

There are seven hydrological parameters in the VIC model which need to be calibrated with recorded daily stream flow. The Nash and Sutcliffe efficiency criterion

(NSE) and the relative error of volumetric fit (RE) were employed as objective functions to calibrate the model (Nash and Sutcliffe, 1970). A good simulation result will have NSE close to 1 and Re close to 0.

2.2 Data Set

The VIC model requires data on soils, vegetation and hydro-meteorology. Vegetation data sets are derived from AVHRR (Advanced Very High Resolution Radiometer, AVHRR) which provide information on global land classification at 1 km resolution. Vegetation parameters, including architectural resistance, minimum stomata resistance, leaf-area index, albedo, roughness length and zero-plane displacement, are derived mainly from LDAS (Land Data Assimilation System, LDAS) (Hansen et al., 2000). The adopted vegetation parameters in the VIC model are listed in the Table 1.

The classification of soil texture is based on global 5-min data provided by the NOAA hydrology office (National Oceanic and Atmospheric Administration, NOAA). The values of soil-related parameters, including porosity, saturated soil potential and saturated hydraulic conductivity, are derived from the work of Cosby et al. (1984) and Raw et al. (1976). The soil parameters used in the VIC model are given in Table 2.

The forcing data used for the VIC model includes daily precipitation, air temperature, solar radiation, vapor pressure and wind velocity. Due to the limited coverage of meteorological data, only daily precipitation and daily maximum and minimum air temperatures are used. There are 2650 meteorological stations in China with available data (among which, 673 stations are from Chinese Meteorology Administration (CMA), 1977 stations are from Ministry of Water Resources (MWR)). Daily precipitation and daily maximum and minimum air temperatures from 1955 to 2008 were collected to drive the VIC model.

As the VIC model is run through grid cells, the whole of China is divided into 4160 cells with a resolution of $0.5^{\circ} \times 0.5^{\circ}$. Meteorological data at 2650 stations were interpolated for each grid cell using a linear distance weighted interpolation method. Daily discharges at the outlet stations of 125 sub-basins in ten major water regions are used

to calibrate and validate the VIC model, and daily discharges at 15 key hydrometric stations on major rivers with large drainage areas are employed to test model performance for large-scale hydrological simulation. The major river system in China and the locations of 125 hydrometric stations on sub-catchments are shown in Fig. 1 Table 3 provides information on the characteristics of the 15 key hydrometric stations on the major rivers.

The selected sub-catchments vary in size and cover different soil, vegetation, morphology, climatic and hydrological characteristics. The area of drainage basins ranges from 284 ~ 87 453 km^2, annual precipitation ranges from 326 ~ 1802 mm, and altitude varies between 41 m to 4452 m. Annual average air temperature varies from −3.6 ~ 22.8°.

3 Results and discussion

3.1 Discharge simulation and regional parameterization

Seven hydrological parameters need to be calibrated with recorded daily stream flow. These are: exponent (B) of variable infiltration curve; depth of each soil layer (d1, d2, and d3); maximum daily base flow (Dm); fractions of base flow; and maximum soil moisture (Ds, Ws) when base flow occurs. Previous studies have documented how some of the major rivers in north China have been highly regulated by intensive human activities since the late 1970s (Xu, 2009; Wang, 2001). In order to eliminate the effects of human activity on runoff, data from 1961–1980 were therefore used to calibrate the model. Thus, the calibrated model parameters should reflect the situation prior to major abstractions and other human influences throughout the basin. Data series were divided into two periods: a period from 1961 to 1975 for model calibration, and a period from 1976 to 1980 for model validation. The simulation results for each sub-catchment, described using the Nash and Sutcliffe efficiency criterion (NSE) and relative error (RE), are illustrated in Figs. 2 and 3 respectively.

Figures 2 and 3 show that the VIC model performs well in general for each catchment. NSEs range from 68.2 % ~ 93.3 % for the calibration period and 61.6 % ~ 92.4 % for the verification period, although NSEs are a little higher in most cases for the calibration period. REs for both periods fall in a small range of −7.1 % ~ +8.2 % with more than 80 % of REs falling in ±5 %.

Based on similarities in climate, soil texture and hydrological features, the calibrated hydrological parameters were transferred to grid cells not covered by the calibrated catchments. In order to test the performance of the VIC model for large scale hydrological simulation with transferred parameter values, the simulated and recorded runoffs at 15 key hydrometric station on major rivers are compared. An illustration of simulated and recorded runoffs for 1961 ~ 1980 at Beipei hydrometric station in southern China, and Tangnaihai hydrometric station in northwest China, is provided in Figs. 4 and 5 respectively.

Figures 4 and 5 show that simulated and recorded runoff closely match for both stations, with about 6.4 % overestimation of low flow on average during the dry season, and about 4.8 % underestimation of peak flow during the flood season. NSEs for both stations exceed 90 % with relative errors of volumtic fit of less than 5 %. Statistical results for monthly discharge simulations of all 15 hydrometric stations on major rivers in China also indicate close correspondence between mean simulated and recorded annual runoff, with relative errors in the water balance of less than 7 %, whlist NSEs are all above 75 %. The transfer of calibrated parameter values to ungauged areas appears to work well in this instance, suggesting that the VIC model works well in simulating runoff across China.

3.2 Climate change scenarios for the next 50 yr

Xu et al. (2005) and Zhang et al. (2006) used the Hadley Centre RCM system-PRECIS (Providing Regional Climates for Impacts Studies, PRECIS) model to analyze changes in temperature and precipitation over the whole China under SRES (Special Report on Emission Scenarios) scenarios A2, B2 and A1B in the 21st century. The projected

country-averaged annual air temperature and precipitation over China under these scenarios 2 are shown in Figs. 6 and 7 respectively.

Figure 6 indicates that projected annual mean air temperatures under the three emission scenarios rise steadily at an annual average rate of approximately 0.045°, with a highest rate of 0.055°/annum under scenario A1B, much higher than previous rates cited by IPCC (IPCC,2007). Figure 7 indicates that annual precipitation is expected to rise slightly, with high variability (from 530 mm annum^{-1} ~ 790 mm annum^{-1}). On average, projected annual precipitations for the period 2021 ~ 2050 increases by 2.1 % ~ 8.7 % compared with the 1961 ~ 1990 baseline.

China's climate varies significantly over time and space because of the influence of topography and monsoon conditions. Projections indicate a significant warming trend across China for the period 2021 ~ 2050, with the largest temperature increases of 1.58° ~ 2.25° and 1.63 ° ~ 2.25° for the Songhuajiang River basin and northwestern part of China. The wetting trend over this period is particularly pronounced in southeast China, the Liaohe River basin, and northwest China, with increases of 5 % ~ 11.2 %, 3.6 % ~ 15.4 % and 4.8 % ~ 13.7 %, respectively, compared to the 1961 ~ 1990 baseline. Drying will probably occur in the Yellow River basin and central China.

3.3 Water resource scenarios for the next 50 yr

China is divided into ten major water regions: Songhuajiang River basin, Liaohe River basin, Haihe River basin, Yellow River basin, Huaihe River basin, Yangtze River basin and Pearl River region (Fig. 1). Based on estimation of synchronous runoff data for a 50 yr period from 1956 ~ 2005, mean annual runoff for China as a whole is 2712 × 10^9 m^3, equivalent to a mean runoff depth of 284 mm. More than 70 % of total runoff occurs in the flood season from June to October in most areas. Southern China accounts for 36.5 % of the geographical area, but has as much as 81 % of total water resources.

The calibrated VIC model was run on 4160 grid cells continuously from 1961 ~ 2050 to estimate runoff at each cell with the projections of RCM-PRECIS under the three SRES emission scenarios of A2, B2, and A1B. Taking runoff in the period 1961 ~ 1990

as a baseline, changes in runoff for the period 2021–2050 for the ten drainage basins listed above were statistically analyzed (Table 4).

Table 4 shows that different scenarios are associated with different changes in annual runoff over China. Scenario A1B projects higher increases in runoff for most areas of China except in the Yellow River basin, with an average increase of 11.3 % for China as a whole, a 2.1 % decrease in the Yellow River basin, and a maximum increase of 20.8 % in the Liaohe River basin. Scenario A2 gives similar results, with the exception of the Songhuajiang River basin where a 4 % decrease in annual runoff is projected. Under scenario B2, annual runoff is projected to decline in most areas of northern China, with a maximum decrease of 10.8 % in Songhuajiang basin.

Changes in runoff during the flood season from June ~ September show similar but more pronounced trends (Table 4). Under scenario A1B, runoff decreases in the Yellow River basin, while other regions experience increases over the same period. Under scenario A2 three regions – the Songhuajiang river basin, the Yellow River basin and northwest China will experience decreasing runoff during the flood season, with the greatest change (a reduction of 7.7 %) in the Yellow River basin. The model suggests other regions will experience an increase in runoff, with the greatest change (an 11.4 % increase) in southeast China.

Taking China as a whole, and with the exception of a 0.7 % decrease in annual runoff under scenario B2, annual runoff will probably increase by between 2.9 % and 11.3 %, and increase by between 0.9 % and 9.1 % for the flood season.

Fig.8 Distribution of projected average runoff changes for annual and flood season from June to September over 2021 ~ 2050 under scenarios of A1B, A2 and B2 (baseline: 1961 ~ 1990)

The spatial distribution of changes in average runoff on an annual and flood season basis (June to September) between the baseline and 2021–2050 under scenarios of A1B, A2, and B2 are shown in Fig. 8. The figure shows that projections are generally similar for the same scenario, but that changes are greater under scenario A1B compared to scenarios A2 and B2. Under all three scenarios, runoff increases in southeast

China and decreases in most of the northeast and central areas, particularly, in the Yellow River basin. Although increases in runoff are projected for most of the northwest under A1B, the opposite occur under A2 and B2. Hence the existing pattern of "North dry and South wet" will likely be exacerbated under global warming.

4 Summary and conclusions

The VIC model with a resolution of $50 \times 50\,km^2$ was calibrated with 125 well-gauged catchments. Based on similarities in climate conditions, soil texture and other properties, model parameters were transferred to non-gauged areas. The VIC model simulates monthly discharge well in different sized catchments, indicating that parameter transfer based on hydrological similarity is a feasible way of implementing regional parameterization of the VIC model across China.

Model results for runoff under different SRES scenarios differ across China. In general, southeast China may experience greater rainfall and runoff in the coming decades, while central China is likely to face greater water scarcity. The pattern of "South wet and north dry" will probably be exacerbated.

Although changes in projected runoff are uncertain, regional water shortages and regional flooding remain key issues that are likely to grow in importance. Climate change will add to the challenges of water resources management by introducing greater variability in water systems and changing flow conditions in surface water systems, amplifying existing patterns of shortage and excess. Effective adaptation strategies will be needed to deal with these trends and safeguard economic growth and poverty reduction efforts under the 12th five-year plan.

Acknowledgements. This study has been financially supported by the National Basic Research Program of China (grant 2010CB951103), the International Science & Technology Cooperation Program of China (grant 2010DFA24330) and the ACCC project funded by DFID, SDC and DECC. Thanks also to the anonymous reviewers and editors.

References

Arnell, N. W.: A simple water balance model for the simulation of stream flow over a large geographic domain [J], J. Hydrol., 217, 314–355, 1999.

Athanasios, L. and Michael, C. Q.: "Effect of climate change on hydrological regime of two climatically different watersheds.", J. Hydrol. Eng., 1(2), 77–87, 1996.

Cosby, B. J.: "A statistical exploration of the relationships of soil moisture characteristics to the physical properties of soils.", Water Resources Res., 20(6), 682–690, 1984.

Ding, Y. H. and Ren, G. Y.: National assessment report of climate change (I): Climate change and its future trend [J], Advances in Climate Change Research, 2(1), 1–8, 2006 (in Chinese with English abstract).

Fu, G. B., Michael, E. B., and Chen, S. L.: "Impacts of climate change on regional hydrological regimes in the Spokane River Watershed.", J. Hydrol. Eng., 12(5), 452–461, 2007.

Gleick, P. H.: The development and testing of a water balance model for climate impact assessment: modeling the Sacramento basin, Water Resour. Res., 23(6), 1049–1061, 1987.

Habets, F., Noilhan, J., Golaz, C., Goutorbe, J.P., Lacarrere, P., Leblois, E., Ledoux, E., Martin, E., Ottle, C., and Vidal-Madjar, D.: The ISBA surface scheme in a macroscale hydrological model applied to the Hapex-Mobilhy area Part I: Model and database, J. Hydrol., 217, 75–96, 1999.

Thodsen, H.: The influence of climate change on stream flow in Danish rivers, J. Hydrol., 333, 226–238, 2007.

Intergovernmental Panel on Climate Change (IPCC): Climate Change and Water. IPCC Technical Paper VI, edited by: Bates, B., Kundzewicz, Z. W., Wu, S., and Palutikof, J., Cambridge, UK and New York, USA: Cambridge University Press, 2008.

IPCC: Climate Change 2007: The Physical Science Basis [M], Cambridge, UK, Cambridge University Press, 2007.

Li, L., Hao, Z. C., Wang, J. H., Wang, Z. H., and Yu, Z. B.: Impact of future climate change on runoff in the head region of the Yellow River, J. Hydrol. Eng., 13(5), 347–354, 2008.

Liang, X. and Xie, Z.: "A new surface runoff parameterization with subgrid-scale soil heterogeneity for land surface model.", Adv. Water Res., 24(1), 173–193, 2001.

Liang, X., Lettenmaier, D. P., Wood, E. F.: "A simple hydrological model of land surface water and energy fluxes for general circulation models", J. Geophys., 99(D7), 14415–14428, 1994.

Lohmann, D., Raschke, E., and Nijssen, B.: "Regional scale hydrology – I: Formulation of the

VIC-2L model coupled to a routing model.", Hydrol. Sci. J., 43(1), 131–141, 1998.
Nash, J. E. and Sutcliffe, J.: River flow forecasting through conceptual models: Part 1 – A discussion of principles, J. Hydrol., 10, 282–290, 1970.
Rawls, W. and Yates, P.: Calibration of Selected Infiltration Equations for the Georgia Coastal Plain. US Department of Agriculture, Agricultural Research Service, 113, Washington, DC, USA, 1976.
Roger, N., Francis, H. S., Walter, C., and Zhang, L.: "Estimating the sensitivity of mean annual runoff to climate change using selected hydrological models." Adv. Water Resour., 29, 1419–1429, 2005.
Huntington, T. G.: Climate warming could reduce runoff significantly in New England, USA, Agr. Forest Meteorol., 117, 193–201, 2003.
Wang, G. Q., Jia, X. A., Chen, J. N., Zhang, Y., Li, H. B., and Wang, Y. Z.: "Analysis on the transition point of hydrological series impacted by human activities – a case study of Wudinghe basin in the middle reaches of the Yellow River.", J. Water Res. and Water Eng., 12(3), 13–15, 2001.
Xu, J. H., Li, X. Y., Chen, J. J., Gao, Y. J., and Li, M.: Impact of Water Conservancy Projects on Storm Flood and Sediment Yield in the Middle Reaches of the Yellow River, Yellow River Press, Zhengzhou, China, 2009.
Xu, Y. L., Huang, X. Y., and Zhang, Y.: Statistical analyses of climate change scenarios over China in the 21st century, Advances in Climate Change Research, 1(2), 80–83, 2005.
Zhang, J. Y. and Wang, G. Q.: Impacts of Climate Change on Hydrology and Water Resources. Science Press, Beijing, China, 2007.
Zhang, J. Y., Wang, G. Q., He, R. M., and Liu, C. S.: "Variation trends of runoffs in the Middle Yellow River basin and its response to climate change.", Adv. Water Sci., 20(2), 153–158, 2009.
Zhang, Y., Xu, Y. L., and Dong, W. J.: A future climate scenario of regional changes in extreme climate events over China using the PRECIS climate model, Geophys. Res. Lett., 33, L24702, doi:10.1029/2006GL027229, 2006.

Table 1. Vegetation-related parameters in VIC model.

	Vegetation classification	Albedo	Minimum stoma resistance (sm^{-1})	Leaf-area index	Roughness length (m)	Zero-plane displacement (m)
1	Evergreen needle leaf forest	0.12	250	3.40 ~ 4.40	1.4760	8.040
2	Evergreen broad leaf forest	0.12	250	3.40 ~ 4.40	1.4760	8.040
3	Deciduous needle leaf forest	0.18	150	1.52 ~ 5.00	1.2300	6.700
4	Deciduous broad leaf forest	0.18	150	1.52 ~ 5.00	1.2300	6.700
5	Mixed forest	0.18	200	1.52 ~ 5.00	1.2300	6.700
6	Woodland	0.18	200	1.52 ~ 5.00	1.2300	6.700
7	Wooded grassland	0.19	125	2.20 ~ 3.85	0.495	1.000
8	Closed shrub land	0.19	135	2.20 ~ 3.85	0.495	1.000
9	Open shrub land	0.19	135	2.20 ~ 3.85	0.495	1.000
10	Grassland	0.2	120	2.20 ~ 3.85	0.0738	0.402
11	Crop land (corn)	0.10	120	0.02 ~ 5.00	0.0060	1.005

Table 2. Soil-related parameters in VIC model.

	Soil texture	2b+3	Bulk density (Kg m^{-3})	θ_s(m^3 m^{-3})	ψ_s	Ks (mm day^{-1})
1	Sand	11.20	1490	0.445	0.069	92.45
2	Loamy sand	10.98	1520	0.434	0.036	1218.24
3	Sandy loam	12.68	1570	0.415	0.141	451.87
4	Silt loam	10.58	1420	0.471	0.759	242.78
5	Silt	9.10	1280	0.523	0.759	242.78
6	Loam	13.60	1490	0.445	0.355	292.03
7	Sandy clay loam	20.32	1600	0.404	0.135	384.48
8	Silty clay loam	17.96	1380	0.486	0.617	176.26
9	Clay loam	19.04	1430	0.467	0.263	211.68
10	Sandy clay	29.00	1570	0.415	0.098	623.81
11	Silty clay	22.52	1350	0.497	0.324	115.78
12	Clay	27.56	1390	0.482	0.468	84.15

Table 3. Basic information of typical river basins used for model performance test.

No.	River	Gauging site	Longitude	Latitude	Area (km^2)	data series
1	Songhuajiang River	Yilan	129.55°	46.33°	491706	1956–2008
2	Songhuajiang River	Ha'erbin	126.58°	45.77°	389769	1956–2008
3	Liaohe River	Tieling	123.83°	42.33°	120764	1956–2008
4	Haihe river	Luanxian	118.75°	39.73°	44100	1956–2008
5	Haihe River	Shixiali	114.62°	40.22°	23627	1956–2008
6	Yellow River	Lanzhou	103.82°	36.07°	229224	1956–2008
7	Yellow River	Huaxian	109.77°	34.58°	106498	1956–2008
8	Huaihe River	Wangjiaba	115.60°	32.43°	30630	1956–2008
9	Huaihe River	Wujiadu	117.38°	32.93°	121330	1956–2008
10	Yangtze River	Shigu	99.93°	26.90°	244489	1956–2008
11	Yangtze River	Beipei	106.42°	29.85°	156142	1956–2008
12	Yangtze River	Huangzhuang	112.58°	31.20°	142056	1956–2008
13	Pearl River	Tian'e	107.17°	25.00°	105535	1956–2008
14	Pearl River	Gaoyao	112.47°	23.05°	351535	1956–2008
15	Minjiang River	Zhuqi	119.10°	26.15°	54500	1956–2008

Table 4. Changes in runoff for 2021 ~ 2050 under scenarios A1B, A2, B2.

No.	River Basin	Changes in annual runoff			Runoff change in Jun–Sep		
		A2	B2	A1B	A2	B2	A1B
I	Songhuajiang River basin	−4.0	−10.8	1.1	−5.5	−11.7	1.4
II	Liaohe River basin	2.6	−6.4	20.8	1.5	−7.4	21.4
III	Haihe River basin	5.2	−3.3	11.3	3.3	−7.7	10.3
IV	Yellow River basin	−4.1	−6.4	−2.1	−7.7	−10.8	−4.2
V	Huaihe River basin	6.0	−1.2	12.9	6.1	−3.1	10.5
VI	Yangtze River basin	6.6	0.7	8.2	8.2	3.1	4.2
VII	Region of southeast China	9.1	8.3	13.2	11.4	12.0	12.3
VIII	Pearl River basin	0.9	−3.0	11.8	0.5	1.1	10.1
IX	Region of southwest China	0.8	0.3	3.6	0.7	−0.4	4.6
X	Region of northwest China	0.2	2.4	2.6	−0.9	2.4	0.6
	China as a whole	2.9	−0.7	11.3	3.4	0.9	9.1

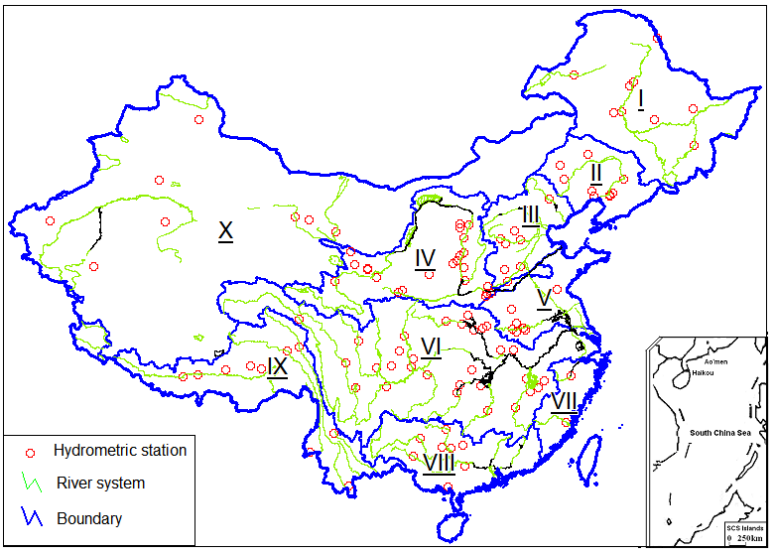

Fig. 1. Major river system in China and locations of sub-catchments for model calibration.

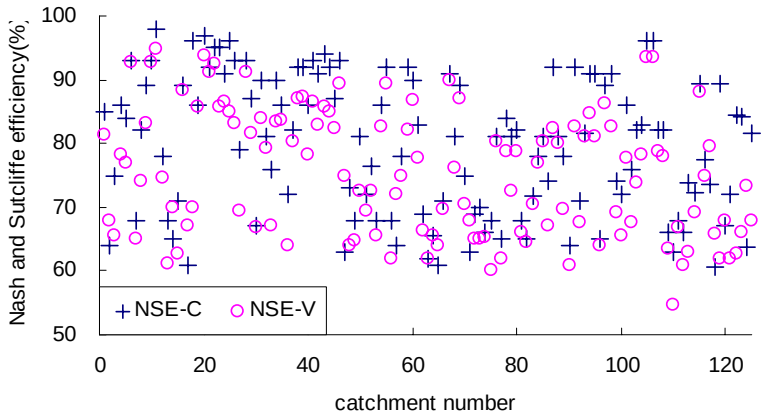

Fig. 2. Nash and Sutcliffe efficiency criterion for each sub-catchment in the calibration period and validation period (NSE-C: Nash and Sutcliffe efficiency criterion in calibration period, NSE-V: Nash and Sutcliffe efficiency criterion in validation period).

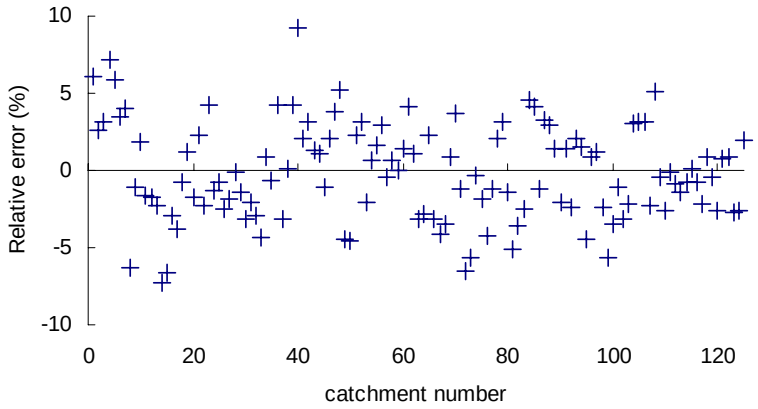

Fig. 3. Relative error of volumetric fit for each site.

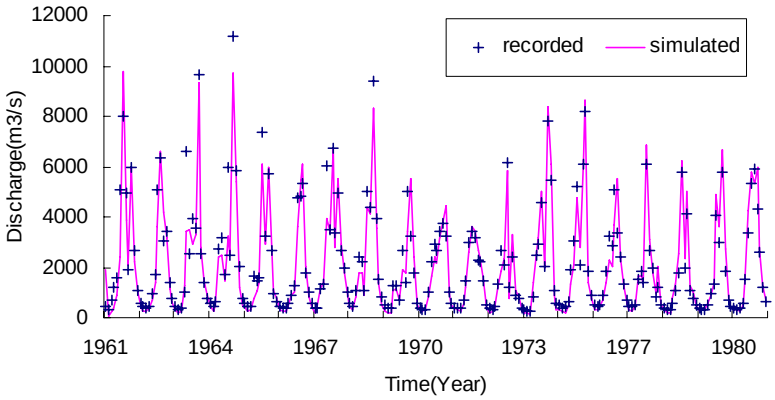

Fig. 4. Recorded and simulated monthly discharge at Tangnaihai station of the Yellow River basin with a drainage area of 121 972 km^2 (NSE = 0.90, RE = −4.2 %).

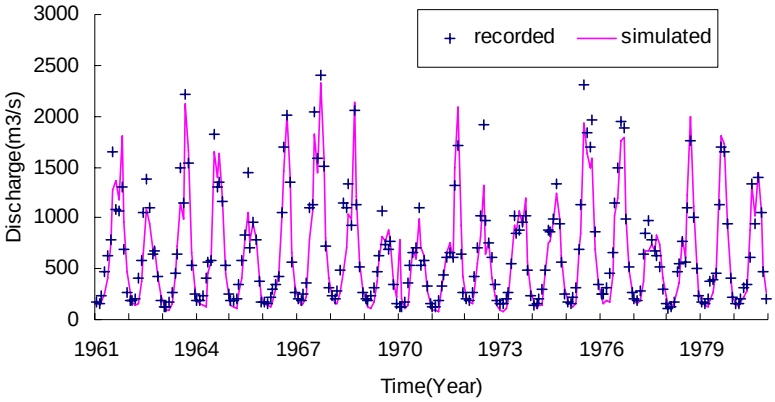

Fig. 5. Recorded and simulated monthly discharge at Beipei station of the Yangtze River basin with a drainage area of 156 142 km^2 (NSE = 0.92, RE = −3.7 %).

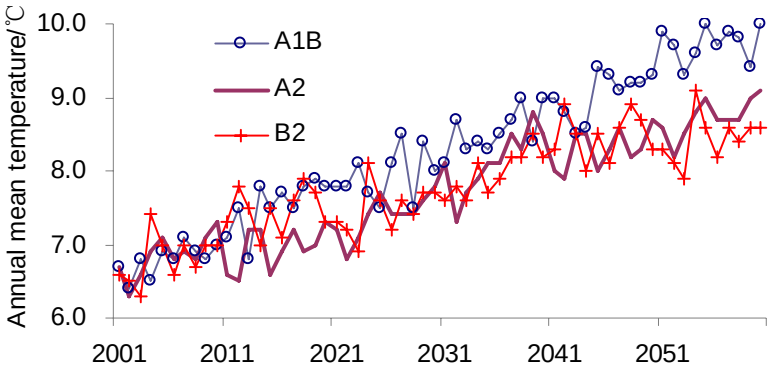

Fig. 6. Projected annual mean air temperature over China under emission scenarios A1B, A2, and B2.

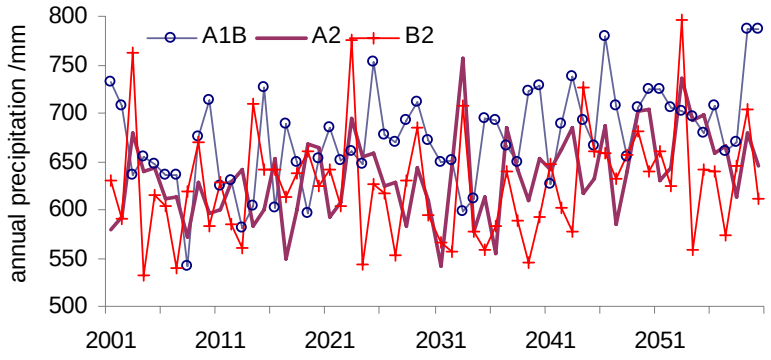

Fig. 7. Projected annual precipitation over the China under emission scenarios A1B, A2, and B2.

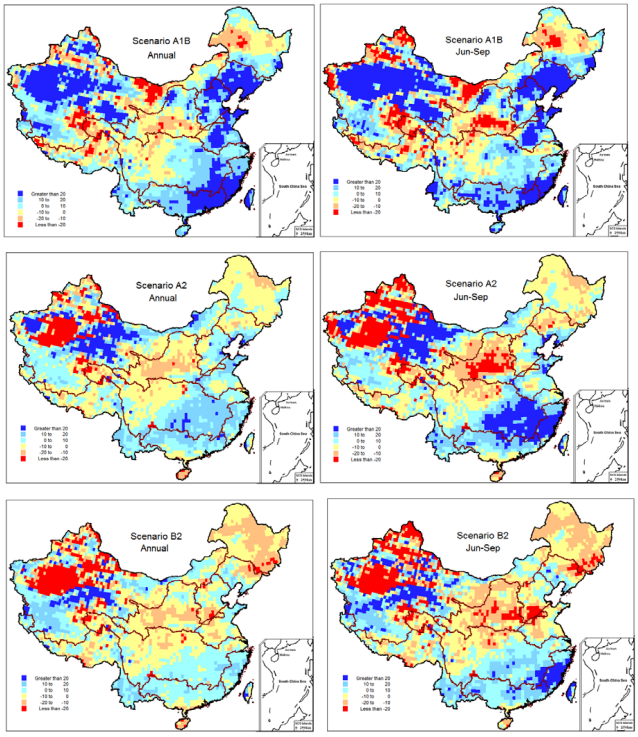

Fig. 8. Distribution of projected average runoff changes for annual and flood season from June to September over 2021 ~ 2050 under scenarios of A1B, A2 and B2 (baseline: 1961 ~ 1990).